Distribution of Sediments Beneath the Ross Ice Shelf, Antarctica from Airborne Magnetic Data

Joel A. Wilner[1], Kirsty J. Tinto[2], Robin E. Bell[2]

[1]*Middlebury College, 14 Old Chapel Road, Middlebury, VT 05753, USA*
[2] *Lamont–Doherty Earth Observatory of Columbia University, 61 Route 9W, Palisades, NY 10964, USA*

Abstract

Knowledge of the tectonic development of the Ross Embayment can help constrain both the development of the West Antarctic Rift and the paleo-erosive extent of the Antarctic Ice Sheet. Thorough understanding of this tectonic development has been hampered by a lack of data constraining the region under the Ross Ice Shelf. In 2015, the first phase of the ROSETTA-Ice mission obtained an extensive suite of aerogeophysical data over the Ross Ice Shelf including radar, lidar, gravity, and magnetics. We applied a Werner deconvolution to the ROSETTA-Ice magnetic data to identify the basement topography below the Ross Ice Shelf. Interpretation of the depth solution was guided by comparison of Werner depth solutions from Operation IceBridge magnetic data in the Ross Sea with the acoustic basement from the ANTOSTRAT project. We established a threshold of susceptibility that provides a good fit between depth estimates of acoustic and magnetic basement. Operation IceBridge and ROSETTA-Ice data were compared along a coincident survey line and found to match well.

We identify a pattern of alternating sediment troughs and highs that can be traced from the Ross Sea underneath the shelf. Notably, we find the Eastern Basin to extend southward from the shelf front for 250 km before curving southeastward, attaining a maximum depth of about 6 km. The Central Trough and Coulman High both extend south-southeastward from the shelf front for 150 km before being truncated by a deep (5-7 km) sedimentary basin that strikes northeastward from the outlet of the Byrd Glacier. We also identify a cross-cutting feature characterized by thick sediments, shallow bathymetry and high free-air gravity, potentially a remnant grounding line of the West Antarctic Ice Sheet. We generally observe thicker sediment at bathymetric highs and thinner sediment at bathymetric troughs, suggesting that the landscape under the Ross Ice Shelf has been significantly influenced by erosion. Despite the thick sediments predicted from the magnetic data, gravity models suggest relatively high densities under these bathymetric highs. Complex relationships between rifting, sedimentation and the resulting gravity anomalies have been reported from the western Ross Sea. Further work will incorporate the ROSETTA-Ice surveys from the 2016 season to investigate these relationships.

I. Introduction

Ice shelves are floating extensions of continental glacial outflow to the ocean, typically ranging from 100 to 1000 meters in thickness. Most ice shelves are located in Antarctica including the Ross Ice Shelf (RIS). The RIS is the largest ice shelf on Earth at 487,000 km^2, located along with the Ross Sea in a large embayment, the Ross Embayment, which cuts into the Antarctic continent (Fig 1). In November-December 2015, the first phase of the ROSETTA-Ice mission, led by Lamont-Doherty Earth Observatory, was conducted. This multi-institutional effort obtained radar, lidar, gravity, and magnetic data over the RIS. A gridded array of flights, comprised of 36 latitudinal transverse lines and 9 longitudinal tie lines, cover a partial area of the RIS and provide a preliminary framework for the geophysical assessment of the RIS (Fig. 2). All remaining ROSETTA-Ice flights will be flown in 2016 to complete the collection of data over the entirety of the RIS.

The areas under the RIS and Ross Sea, along with the area of West Antarctica extending between Marie Byrd Land and the base of the Antarctic Peninsula, comprise the West Antarctic Rift System, a large, mid-late Cretaceous (105-85 Ma) rifting zone comparable in size to the Basin and Range and East African rift systems (Behrendt et al., 1991). It is well established in the literature through a variety of geophysical means that sedimentary basins from Cretaceous rifting underlie the Ross Sea (Davey et al.1983, Karner et al. 2005, Bell et al., 2006). The three major southerly sedimentary basins are, from east to west, the Eastern Basin, the Central Trough, and the Victoria Land Basin (Fig. 3). Between these sedimentary basins are two basement highs, the Central High and the Coulman High. The Transantarctic Mountains likely form the entire shoulder of the rift province, rising to a maximum height of 5 km. It is generally interpreted that the Transantarctic Mountain began uplift during the early Paleogene (60 Ma) (Behrendt and Cooper, 1991). Paleogene-Neogene rift reactivation resulted in the Terror Rift, a linear, narrow rift in the western Ross Sea (Cooper et al., 1987).

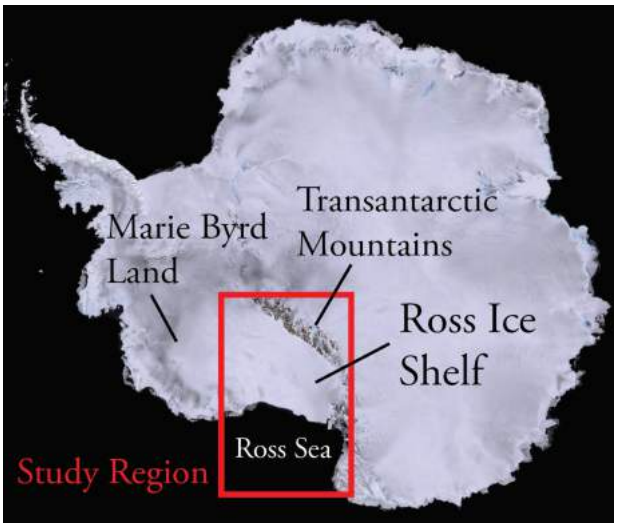

Fig. 1. The location of the Ross Embayment (the RIS and Ross Sea) relative to the Antarctic continent.

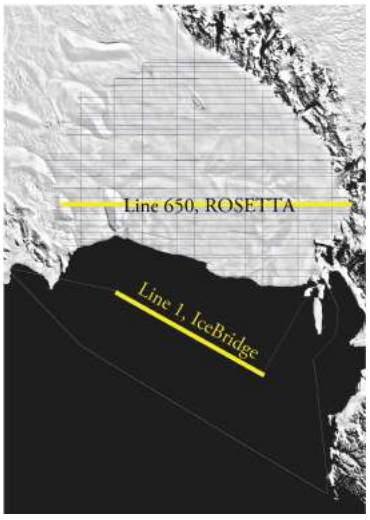

Fig 2. ROSETTA-Ice flight grid over the Ross Sea and Operation IceBridge flight lines in the Ross Sea, with comparison lines highlighted.

To date, it has been assumed that the sedimentary basins of the Ross Sea continue underneath the RIS parallel to the Transantarctic Mountains in the Ross Sea. However, no direct evidence has ever been provided to support this assumption. Little is known about the nature of rifting beneath the RIS or the underlying bedrock structures, both of which have significant implications for the formation of the West Antarctic Rift as a whole, as well as the erosive extent of the Antarctic Ice Sheet during past fluctuations. A primary component of this study involves assessing which structures beneath the RIS are tectonic in origin and which structures erosive in origin. This study involves the analysis of magnetic data from the first phase of the ROSETTA-Ice mission to provide the first direct interpretation of crustal structure and extensional sedimentary basins beneath the RIS.

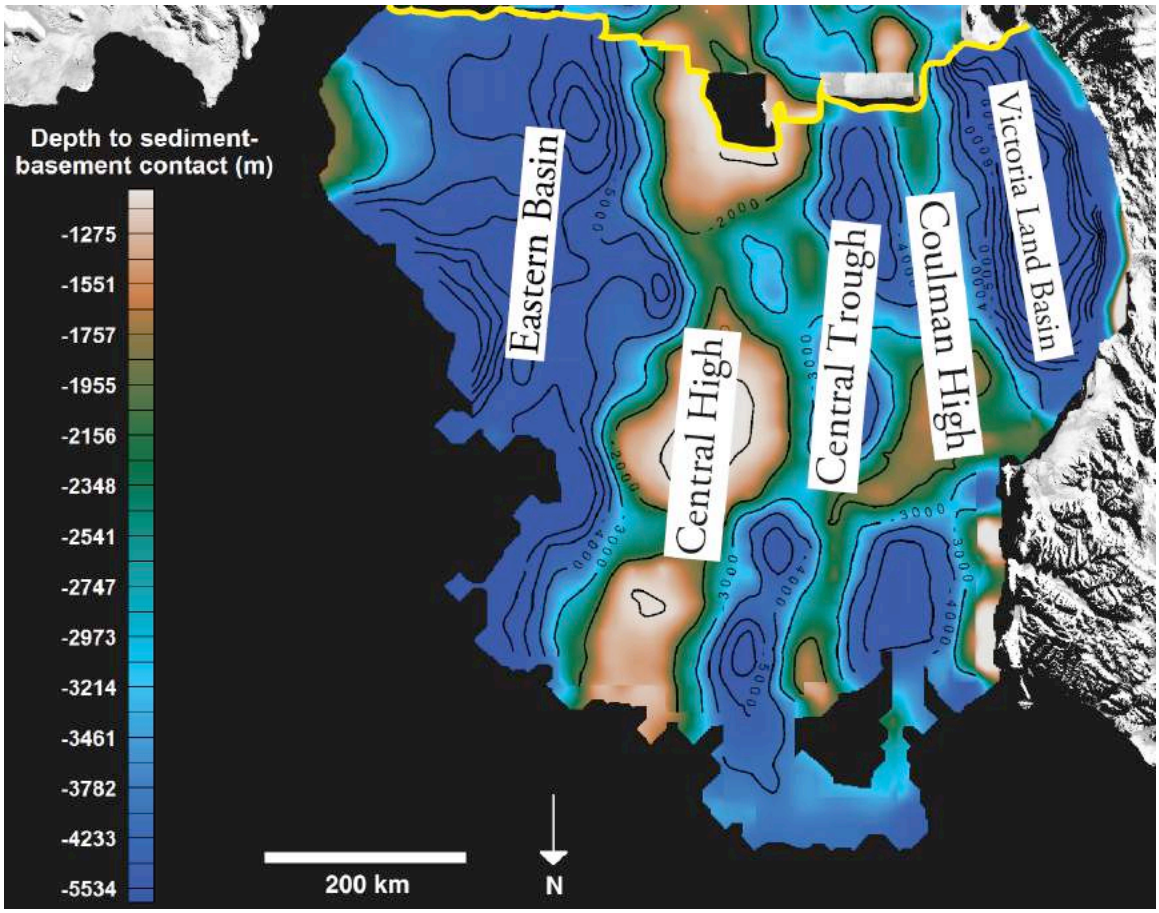

Fig. 3. Below yellow line, major sediment basins and crustal highs underneath the Ross Sea. From seismic depth to acoustic basement ANTOSTRAT data (ANTOSTRAT Project, 1995).

2. Methodology

2.1. Instrumentation

The 2015 ROSETTA-Ice flights utilized a Lockheed C-130 Hercules aircraft over the RIS to obtain aerogeophysical data. The 8.5-foot long by 2-foot wide icePod is a modular pod system containing science imaging and positioning instruments (lidar, depth sounding radar, high-resolution visible wave camera, thermal infra-red camera, infrared radiation pyrometer, global navigation satellite system, shallow ice sounding radar, magnetometer, gravimeter, conductivity-temperature-depth sounders, and atmospheric chemistry sensors). The two primary icePod instruments used in this study are the magnetometer and gravimeter. The magnetometers in icePod include a Scintrex CS-3 cesium vapor magnetometer and a Billingsley TFM100G2 magnetometer, sampling at a rate of 100 Hz to a precision of 0.1 nT. The gravimeters in icePod include a BGM3 gravimeter and an L&R S-80 gravimeter, measuring both free-air gravity anomaly and Bouguer gravity anomaly. The gravimeters sample at a rate of 1 Hz with an accuracy of approximately 2 mGal and an along-track resolution of 14 km assuming a 170 s filter. The typical surveying altitude of the aircraft is 3000 AGL, surveying at 170 knots (ground speed).

2.2. Magnetic Susceptibility

Magnetic susceptibility, a dimensionless property, is defined as the ratio between induced magnetization and the intensity of the externally applied magnetic field (Petrovsky and Kapika, 2006). Simply, magnetic susceptibility is a measure of how easily a material can be magnetized. The magnetic field of Earth induces magnetism in rocks containing magnetic minerals like magnetite or ilmenite and, generally, the mineralogy of igneous materials favors higher magnetic susceptibility than the mineralogy of sedimentary materials. For example, igneous rocks have an average magnetic susceptibility of 2.69 and sedimentary rocks have an average magnetic susceptibility of 2.19 (Hunt et al., 1995). As a result, the crystalline crustal basement beneath the RIS carries a higher average susceptibility than the overlying sedimentary infill layer.

2.3. Werner Deconvolution

In geophysical models, the appropriate model for the depth-to-source of a magnetic anomaly uses the magnetic anomaly given by a dike or sill. A dike or sill may refer to a true igneous dike or sill with a higher magnetic susceptibility than surrounding the bedrock. More commonly, though, the causative source of the “dike” or “sill” is actually the contact between the crystalline bedrock basement with an upper layer, often unconsolidated or partially consolidated sediment (Birch, 1984).

Werner (1953) proposed a technique to estimate the depth to basement for sheet- or sill-like (contact) and dike-like bodies. This technique, now called the Werner deconvolution, isolates the field contributed by a particular dike or contact from neighboring dikes or contacts. It can be considered an inverse technique in that we first observe the magnetic field and subsequently solve for the source parameters of the

causative body. Birch (1984) outlined the basic mathematical process of the Werner deconvolution technique employed by potential field software packages, summarized here. The magnetic anomaly h, in nT, of the dike- or sheet-like body is approximated by

$$h = 2H\ ktz/[z^2 + (x - x_0)] \tag{1}$$

where H is the magnetic field of the Earth given in nT, k is the dimensionless magnetic susceptibility of the causative body, t is the modeled lateral thickness of the causative body given in meters, z is the vertical distance of the sensor from the causative body given in meters, x is the horizontal distance of the sensor from the start of the profile given in meters, and x_0 is the horizontal distance of the center of the causative body from the start of the profile given in meters. Equation (1) is algebraically rearranged to obtain the equation

$$a_0 h + a_1 + a_2 hx = hx^2 \tag{2}$$

where a_0, a_1, and a_2 are unknown constants that are related to the desired parameters x_0, kt, and z by

$$x_0 = a_2/2 \tag{3}$$

$$kt = a_1/2H\sqrt{-a_2^2/4 - a_0} \tag{4}$$

$$z = \pm\sqrt{-a_2^2/4 - a_0} \tag{5}$$

The potential field software runs equation (2) through three successive points on the magnetic anomaly profile, where h and x are known, and solves the system of three equations for a_0, a_1, and a_2. These constants are then used to solve for the desired parameters x_0, kt, and z from equations (3)-(5). These parameters relate the horizontal location, susceptibility, and depth of each Werner solution, respectively. The program then shifts the three successive points over a given interval until it completes the entire length of the magnetic anomaly profile, giving Werner solutions throughout the profile.

This research applies a Werner deconvolution to the ROSETTA-Ice magnetic data to identify the boundary between the sedimentary sequence and basement rock beneath the RIS. We use the Werner Deconvolution GX program implemented in the potential field software Geosoft Oasis montaj to compute depth-to-source estimates. Because the geometry of the magnetic source is unknown, Werner solutions for both dikes and sheets (referred to as "contacts" in Geosoft Oasis montaj) are both considered in this study. The Werner Deconvolution GX program in Geosoft Oasis montaj allows the user to specify the minimum and maximum window size for equation (1) of the Werner calculation as it proceeds through the anomaly profile, along with an increment for the program to increase the window size with each successive calculation. The calculation uses the smallest window size for one run from the beginning to the end of the anomaly profile, then increments the window size based on the user-specified input and reprocesses the entire profile. This procedure continues until the profile has been processed using the

user-specified maximum window size. We find that the following Werner deconvolution parameters in the Werner Deconvolution GX program in Geosoft Oasis montaj provide physically realistic solutions for the RIS: Minimum Depth 800 m; Maximum Depth 9000 m; Minimum Window Length 1000 m; Maximum Window Length 10000 m; Window Expansion Increment 1000 m; Window Shift Increment 1000 m.

Werner deconvolution was applied to all ROSETTA-Ice flight lines. Automated clustering of Werner solutions was attempted initially but found to produce unrealistic results. Consequently, the sediment-basement contact was picked manually using the GM-SYS profile modeling program.

2.4. Assessment of Confidence in the Werner Deconvolution Method

To assess the viability of the Werner deconvolution method to identify the sediment-basement boundary, the Werner deconvolution was applied to magnetic data from line 1 of Operation IceBridge in the Ross Sea (Fig. 2). The resulting Werner solutions were compared with a coincident profile from ANTOSTRAT seismic data of depth to basement (Fig. 4).

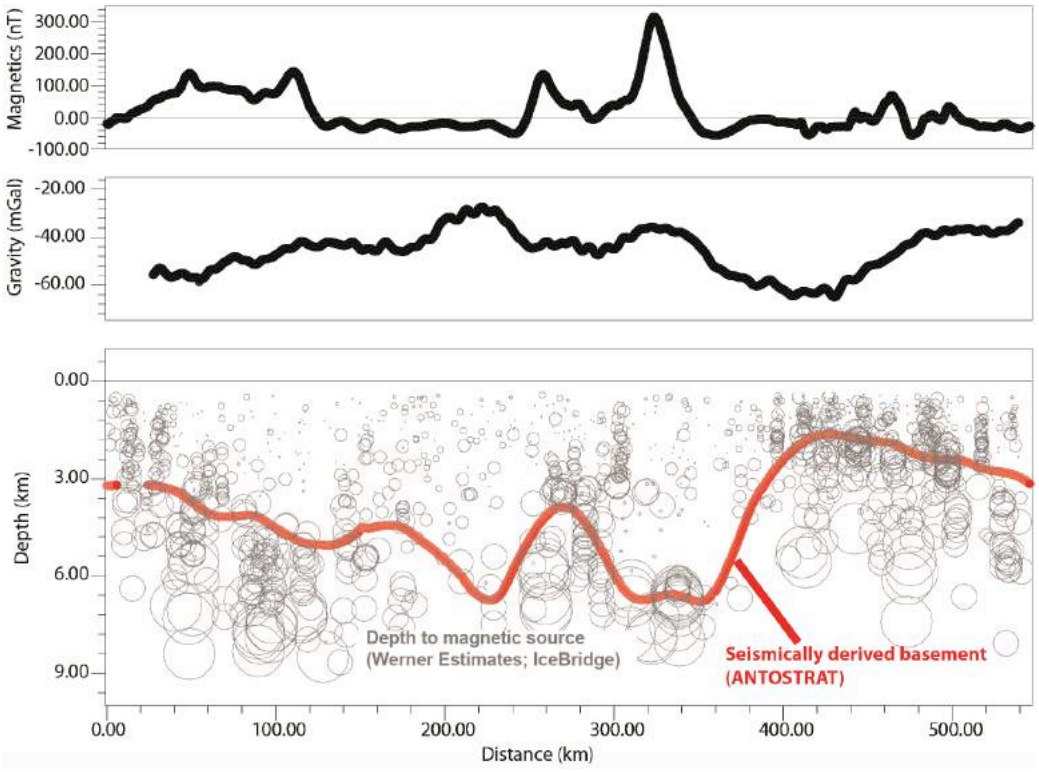

Fig. 4. Depth to magnetic basement vs. depth to acoustic basement. Werner solution circles from Operation IceBridge line 1 in the Ross Sea are scaled in size to magnetic susceptibility. Bold line is ANTOSTRAT acoustic basement. Magnetic and gravity profiles for Operation IceBridge line are shown.

In Fig. 4, the close correlation between the tops of high-susceptibility streaks and the ANTOSTRAT acoustic basement along the same profile demonstrates the ability of the Werner Deconvolution GX program in Geosoft Oasis montaj to identify the sediment-basement contact from Operation IceBridge data. The Werner depth estimates tend to cluster vertically below the actual location of the causative body, here interpreted as the sediment-basement contact from ANTOSTRAT data. This vertical clustering is consistent with applications of Werner deconvolution in the Ross Sea elsewhere in the literature (Karner et al., 2005). A statistical measurement of confidence will be useful to quantify in the future.

With confidence having been established in Werner deconvolution method to identify the sediment-basement contact from Operation IceBridge data, a Werner deconvolution was applied to Line 650 of the ROSETTA-Ice flights, coincident with a line from Operation Ice Bridge (Fig. 2). Agreement between the two profiles would transitively establish confidence in the Werner deconvolution method to identify the sediment-basement contact from ROSETTA-Ice magnetic data. The resulting profile comparison shows close agreement between the Operation IceBridge solutions and ROSETTA-Ice solutions and demonstrates the ability of the Werner deconvolution to identify the sediment-basement contact in ROSETTA-Ice data (Fig. 5). Accordingly, the nature of agreement between ANTOSTRAT and Operation IceBridge profiles and between Operation IceBridge and ROSETTA-Ice profiles served as the benchmark by which ROSETTA-Ice solutions were manually picked. A minimum susceptibility threshold of 1 was determined upon inspection of the magnetic-acoustic basement agreement (solutions of lesser susceptibility showed little agreement between solution profiles) and was applied to ROSETTA-Ice solutions prior to picking the sediment-basement contact.

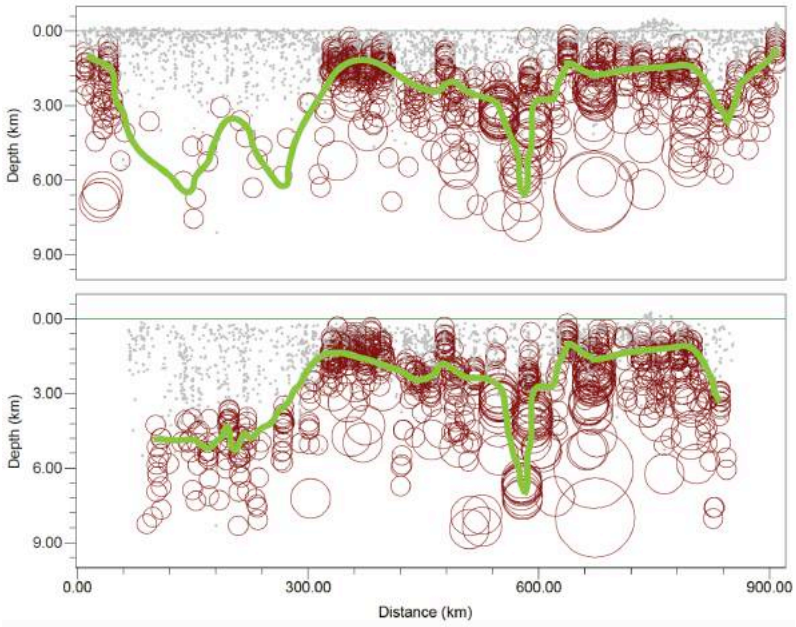

Fig. 5. Werner deconvolution solutions for (top) Line 650 of ROSETTA-Ice and (bottom) the coincident Operation IceBridge line. Solutions of susceptibility ≥ 1 are scaled in size to susceptibility; solutions of susceptibility < 1 are shown as dots. Green line indicates manually picked sediment-basement contact. First ~75 km and final ~90 km of Operation IceBridge line are not included because data were not collected over those intervals.

3. Results

Gridding of manually picked Werner solutions results in the first depth to sediment-basement contact map produced for the RIS (Fig. 6). Supplementary maps from various datasets collected in ROSETTA-Ice and RIGGS projects have also been gridded, providing a set of maps for comparison of broad-scale trends in the RIS region (Fig. 7a-7f).

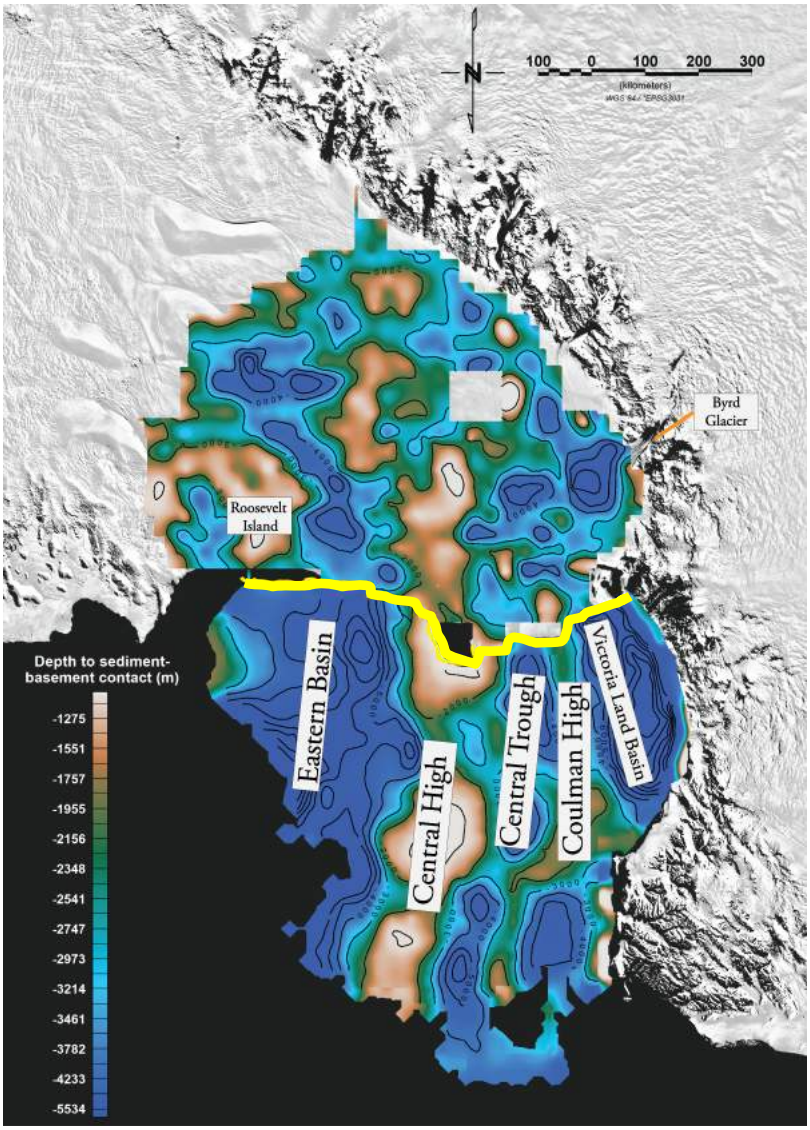

Fig. 6. Depth to sediment-basement contact from the ellipsoid for the RIS determined by Werner deconvolution picking method from ROSETTA magnetic data (above yellow line); depth to sediment-basement contact from sea level for the Ross Sea determined by ANTOSTRAT seismic data (below yellow line) (ANTOSTRAT Project, 1995). Major Ross Sea sediment basins and crustal highs are labeled; other features of note are labeled.

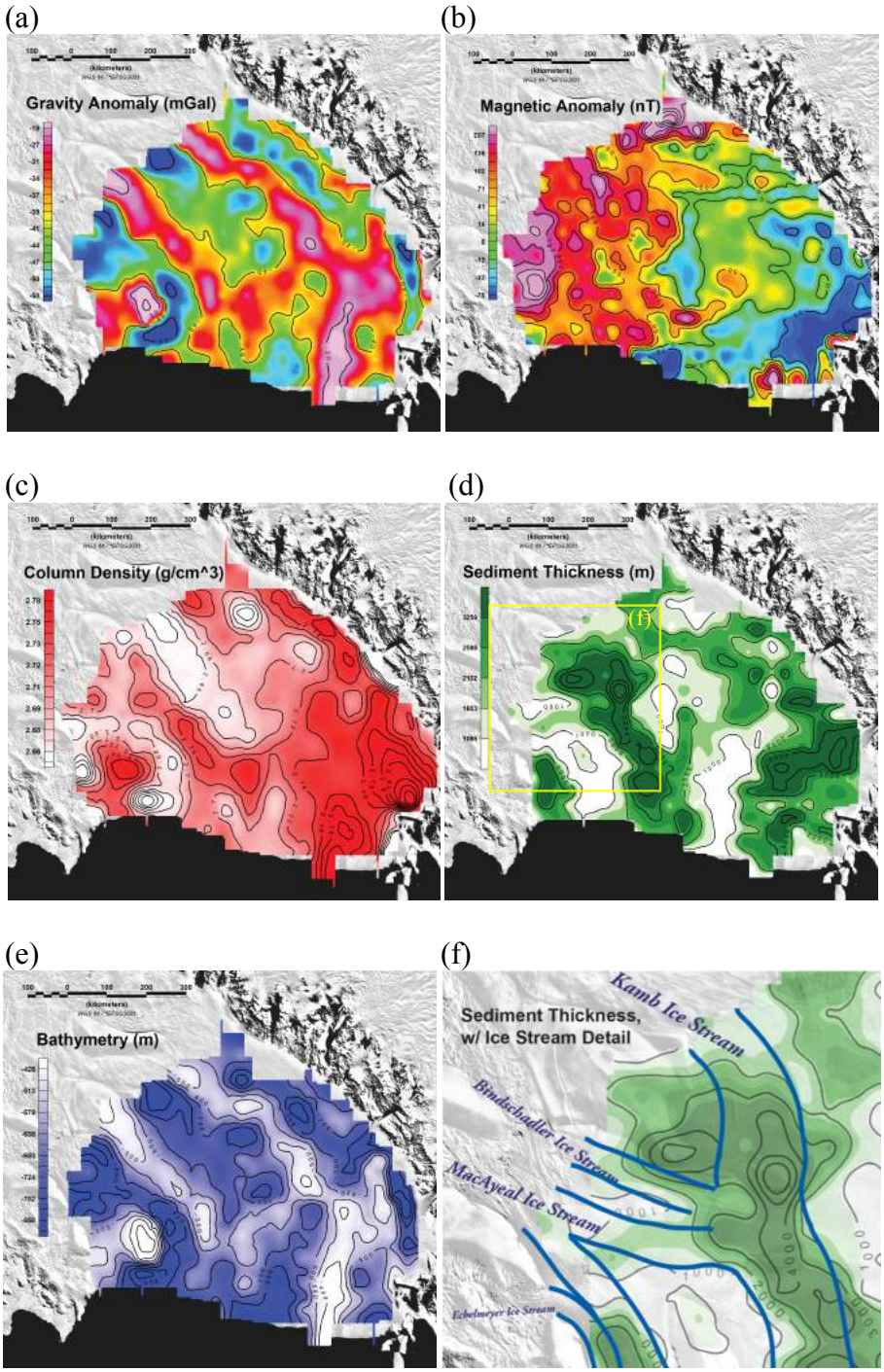

Fig. 7. Gridded RIS maps primarily from ROSETTA-Ice datasets. (a) Free-air gravity anomaly over the RIS (ROSETTA data). (b) Magnetic anomaly over the RIS (ROSETTA). (c) 10 km vertical column density beneath the seafloor (RIGGS data constrained by ROSETTA) (Thomas et al. 1984). (d) Sediment thickness from seafloor to basement (ROSETTA). (e) Bathymetry underneath the Ross Ice Shelf from gravity inversion (ROSETTA). (f) From inset in (d), detail of sediment thickness with ice stream inflow delineated.

4. Discussion

Because sediment is less dense than crustal material, we expect crustal troughs (filled with more sediment) to exhibit lower columnar density than crustal highs (filled with less sediment). Here, however, we find the opposite to be generally true (Fig. 6, Fig. 7c, Fig. 7d), with the major exception of Roosevelt Island. Considering that crustal troughs under the Ross Ice Shelf are generally coupled with relative peaks in the free-air gravity anomaly (Fig. 6, Fig. 7c) and follow the strike of Ross Sea crustal troughs and then possibly the bend of the Transantarctic Mountains, these results may support the model of very high-density crustal intrusions beneath rift basin depocenters in the Ross Sea discussed by Karner et al. (2005), and that such rifts basins with crustal intrusions extend beneath the ice shelf (Fig. 8). Karner et al. (2005) cast doubt on the crustal intrusion model, arguing that the volume of magma produced during Neogene alkalic volcanism in the Ross Sea region is too small to appreciably increase the density of Ross Sea thinned crust as crustal intrusions. However, the similar anti-correlation between gravity highs and the location of sedimentary basins continues underneath the RIS and covers a larger area than previously known, raising the possibility that a more widespread, previously unconsidered regional mechanism of magmatic intrusion occurred during rifting. This is purely speculative, though, and more detailed structural and geophysical analysis is required. Other studies have attributed the gravity anomaly high over Ross Sea basin depocenters to high-density volcanics within the sedimentary infill (Davey, 1981; Tréhu et al., 1993). Another possibility is that a significant difference between the flexural strength of the lithosphere during rifting and during sedimentation accounts for the gravity high over basin depocenters (Fig. 9) (Karner et al., 2005).

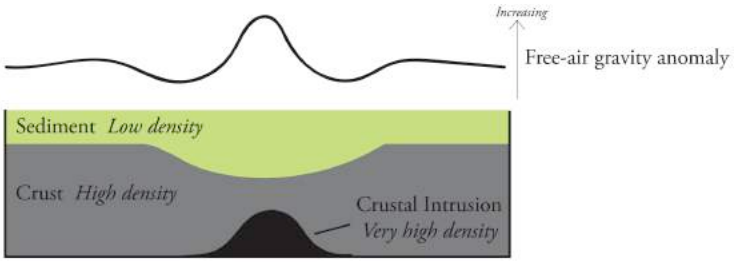

Fig. 8. Simplified model of the free-air gravity anomaly over a sedimentary depocenter-aligned crustal intrusion. Adapted from Karner et al. (2005).

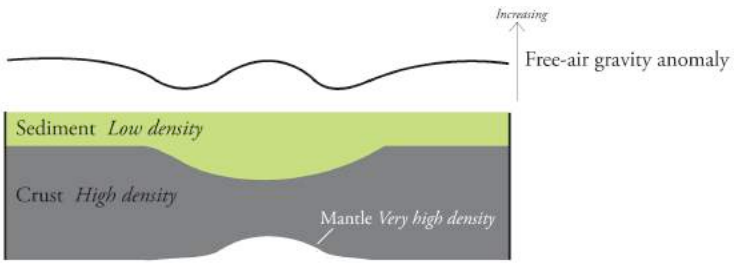

Fig. 9. Simplified model of the free-air gravity anomaly over a sedimentary depocenter in the case of varying lithospheric flexural strengths during rifting and sedimentation. Figure adapted from Karner et al. (2005).

Fig. 6 shows that major extensional features continue underneath the Ross Ice Shelf, which had only been speculated in the past (Karner et al., 2005). Most notably, the Eastern Basin continues south for several hundred kilometers beyond the RIS front (interrupted by Roosevelt Island) before turning southeast towards Siple Dome. The Central High proceeds in a similar fashion, although its direction deeper into the RIS becomes unclear. Although broad and general, this continuation of known rift features supports the notion of extensional rifting beneath the RIS.

The Central Trough and Coulman High extend south-southeastward 100 to 200 km underneath the RIS from its front before being truncated by a deep feature (Fig. 6). This feature is characterized by thick sediments (Fig. 7d) and extends northeast from the outlet of the Byrd Glacier along the general strike of the Byrd Glacier. This may suggest a paleo-erosive extension of the Byrd Glacier cutting into rift features and sediment infill. Notably, the feature is absent in other datasets, including bathymetry, gravity, and magnetics.

A major northwest-southeast striking feature slightly southwest of the center of the RIS appears in several datasets. This cross-cutting feature is characterized by thick sediments, high free-air gravity, high density, and shallow bathymetry, and is roughly parallel to the present-day grounding line of West Antarctica along the RIS (Fig. 6, Fig.7a, Fig.7c, Fig.7d, Fig.7e). This evidence is suggestive of a major paleo-grounding line, the thick sediments and shallow bathymetry consistent with accumulated sediment from grounding line depositional systems. These depositional systems include morainal banks, ice-contact deltas, and grounding-line fans (Powell, 1991).

While it generally understood in the literature that the Ross Embayment encompasses an extensional rifting zone, the extent to which erosion dominates over rifting in the submarine landscape is unclear. We generally observe thicker sediment beneath bathymetric highs and thinner sediment beneath bathymetric troughs under the RIS, suggesting widespread erosive and depositional influence of glacial bodies. Furthermore, the flow paths of several major ice streams coincide with thick sediments (Fig. 7d). It is plausible that rift basins have provided favorable pathways to ice streams of West Antarctica, which have precipitated vast amounts of sediment within rift basins in the Ross Embayment. It is not entirely clear, however, which pathways can be attributed solely to rifting and which solely to paleo-erosion.

5. Conclusions and Suggestions for Future Work

This study provides valuable new information about the basement and sediment structure beneath the RIS, supplementing previous seismic, magnetic, and gravity studies from the Ross Sea. Preliminary Werner deconvolution solutions indicate a basement that generally continues most of the rift patterns observed in the Ross Sea, supporting the notion that the Ross Embayment as a whole, not simply the Ross Sea, is a product of late Cretaceous extensional rifting. The RIS exhibits paradoxically high gravity anomalies over sediment depocenters, similar to those in the Ross Sea discussed by Karner et al. (2005), suggesting that complex relationships exist between rifting and sedimentation in the Ross Embayment. A cross-cutting feature near the center of the RIS characterized by thick sediments and a bathymetric high parallel to the modern-day grounding line of the

West Antarctic Ice Sheet is suggestive of a paleo-grounding line of the West Antarctic Ice Sheet.

We suggest that further analysis and gravity modeling of the paradoxical gravity highs over sediment depocenters be conducted. Data from the second phase of the ROSETTA-Ice flights will be incorporated into this study once they are collected in late 2016. Additionally, development of a method to automatically pick the top of vertically streaked solution clusters of high magnetic susceptibility, rather than manually picking, would improve consistency and accuracy of sediment-basement contact selection. It is also unclear if rift basins beneath the RIS remain parallel to the Transantarctic Mountains, which would have implications for the uplift of the Transantarctic Mountains. Further structural analysis is required.

Acknowledgments

J. Wilner thanks Kirsty Tinto and Robin Bell, as well as the rest of the Polar Geophysics Group at Lamont-Doherty Earth Observatory, for their support and mentorship. Thanks also to the LDEO Summer Intern Program, Dallas Abbott, Operation IceBridge, and the National Science Foundation.

References

ANTOSTRAT Project, 1995. Seismic stratigraphic atlas of the Ross Sea, Antarctica, in: A.K. Cooper, P.F. Barker, G. Brancolini (Eds.), Geology and Seismic Stratigraphy of the Antarctic Margin, Antarct. Res. Ser., vol. 68, AGU, Washington, D.C., p. A271-A286.

Behrendt, J.C., A. Cooper, 1991. Evidence of rapid Cenozoic uplift of the shoulder escarpment of the Cenozoic West Antarctic rift system and speculation on possible climate forcing, Geology 19, p. 315-319.

Behrendt, J.C., W.E. LeMasurier, A.K. Cooper, F. Tessensohn, A. Trehu, and D. Damaske, 1991. Geophysical studies of the West Antarctic rift system, Tectonics 10 (6), p. 1257-1273.

Bell, R., M. Studinger, G.D. Karner, C. Finn, and D. Blankenship, 2006. Identifying major sedimentary basins beneath the West Antarctic Ice Sheet from aeromagnetic data analysis, in Fütterer, D.K., et al., eds., Antarctica: Contributions to Global Earth Sciences: Berlin, Springer, p. 117-121.

Birch, F.S., 1984. Bedrock depth estimates from ground magnetometer profiles. Ground Water 22: p. 427–432.

Cooper, A.K., F.J. Davey, and J.C. Behrendt, 1987. Seismic stratigraphy and structure of the Victoria Land Basin, Western Ross Sea, Antarctica, in: A.K. Cooper, F.J. Davey (Eds.), The Antarctic Continental Margin: Geology and Geophysics of the Western Ross Sea, Earth Sci. Ser., vol. 5B, Circum-Pacific Res. Counc., Houston, TX, p. 119–138.

Davey, F.J., 1981. Geophysical studies in the Ross Sea region, J. R.Soc. N.Z. 11: p. 465–479.

Davey, F.J., K. Hinz and H. Schroeder, 1983. Sedimentary basins of the Ross Sea, Antarctica, in: Antarctic Earth Science, R.L. Oliver, P.R. James and J.B. Jago, eds., Australian Academy of Science, Canberra, AC.T., p. 553-538.

Hunt, C.P., B.M. Moskowitz and S.K. Banerjee, 1995. Magnetic properties of rocks and minerals. In: Ahrens, T.J. (Ed.), Rock Physics and Phase Relations. A Handbook of Physical Constants. American Geophysical Union, p.189–204.

Karner, G.D., M. Studinger, and R. Bell, 2005. Gravity anomalies of sedimentary basins and their mechanical implications: Application to the Ross Sea basins, West Antarctica: Earth and Planetary Science Letters, v. 235, p. 577–596.

Petrovsky, E. and A. Kapicka, 2006. On determination of the Curie point from thermomagnetic curves. Journal of Geophysical Research 111.

Powell, R.D., 1991. Grounding-line systems as second-order controls on fluctuations of tidewater termini of temperate glaciers. In: Anderson, J.B., Ashley, G.M. (Eds.), Glacial Marine Sedimentation: Palaeoclimatic Significance. Geological Society of America Special Paper, vol. 261, p. 75–93.

Thomas, R.H., D.R. MacAyeal, D.H. Eilers, and D.R. Gaylord, 1984. Glaciological Studies on the Ross Ice Shelf, Antarctica, 1972-1978. The Ross Ice Shelf: Glaciology and Geophysics Antarctic Research Series, AGU.

Tréhu, A.M., J.C Behrendt, J.C. Fritsch, 1993. Generalized crustal structure of the Central basin, Ross Sea, Antarctica, in: D. Damaske, J. Fritsch (Eds.), German Antarctic North Victoria Land expedition 1988/89; GANOVEX V, Geol. Jahrb. Reihe E, vol. 47: p. 291– 311

Werner, S, 1953. Interpretation of magnetic anomalies at sheet-like bodies, Sver. Geol. Undersok., ser. C. C. Arsbok., no. 06.